Transient Characteristics Analysis Based-on Circuit Models for a High-Speed Rail System

KUEI-HSIANG CHAO[1], PI-YUN CHEN[1] and CHUN-HSIN CHENG[2]
[1]Department of Electrical Engineering,
National Chin-Yi University of Technology
35, Lane 215, Sec. 1, Chung-Shan Road, Taiping City, Taichung County
TAIWAN, R.O.C.
chaokh@ncut.edu.tw
[2]Institute of Information and Electrical Energy, National Chin-Yi University of Technology

Abstract: - The main purpose of this study is to analyze the current leakage of the power grid due to the change in speed of high-speed rail (HSR). First, using PSIM software as the fundamental basis, this study constructed an overall HSR circuit-based model system, including Scott transformer, auto-transformer, and the track equivalent circuit and grounding system. In addition, this paper sought to study the current leakage transient responses of a train's change in speed using this equivalent circuit model. Through simulation results, the study found that the dramatic change in DC voltage from a change in the speed of electric locomotives causes current leakage flowing through the high-speed rail power grid and a rise in ground potential. The study's analysis results provide possible performance improvements to the high speed rail's electric locomotives during changes in speed.

Key-Words: High-Speed Rail System, Scott Transformer, Leakage Current, Transient Behavior.

1 Introduction

Because the power supply of high-speed railway traction powered vehicles belongs to the power supply category of "high-capacity rapid transit systems," when these vehicles accelerate, the current needed increases dramatically. Therefore, an "overhead AC power supply system" is often used. The way this system works, is that the traction power substation first feeds electricity to the catenary line and negative feeder line; then the power train using pantograph to capture the AC power generated between the tough wire and the railway to supply power for the vehicle. Because the load carried on the high speed rail changes frequently, voltage changes in the power supply system will be induced. In addition, voltage drops in the power supply system can be induced when the tough line short-circuits or is grounded [1]. The degree of these voltage changes must be within a certain range that the system can tolerate, otherwise, there will be negative effects on general users.

Due to the high speed rail vehicle uses AC motor as the driving motor, the inverter is used to control the train's speed. However, the inverter, using the pulse width modulation (PWM) technique caused by the common-mode voltage, combined with the leakage current generated by motor winding and the shell's inner region's stray electricity, causes leakage current to increase and ground potential to rise [2,3]. This subsequently leads to the system's grounding fault protection relay to be stripped [4-6] and at the same time causes electric corrosion to the railway [7], furthering the motor's damage to the vehicle's system. Thus, when constructing the high speed rail's power grid and other electric circuit routes, it is important to look at the situations of the high speed rail's vehicle during its speed changes and the effects of the leakage current generated on the power grid.

This paper will focus on the speed changes of the high speed rail's vehicle and the effects this process has on the leakage current of the power grid. First, the PSIM software was used to establish the basic fundamental high speed rail's power supply system network, which included a main transformer of the high speed rail, local transformer, and the equivalent circuit of the rail and grounding system. In addition, this equivalent circuit and three-level neutral point clamped (NPC) AC/DC converter were used to complete the construction of the high speed rail traction drive system for analyzing the transient characteristics of the current leakage behavior during the vehicle's change in speed.

2 The Structure of the Power Supply System Network of High Speed Rail Vehicles

2.1 Structure of the Main Transformer of the Power Supply System Network

The power supply system network of the high speed rail is powered by the primary power substation. First, a three-phase 161kV power system uses a power double loop to feed electricity, then a set of two 50MVA transformers prepared by high speed rail in the power substation transforms the three phase 161kV to two sets of single phase power source. The distance between power substations is a maximum of 60km. This design allows for the power supply of the high speed rail to maintain good normal operation even if any one transformer exhibits problems.

In a three-phase power system, if the needed power is instead single phase, there will be an imbalance in the voltages in the power supply system network. To solve this problem, a connection can be made at the traction power supply substation using many different methods, including the single phase direct connection method, V-connected method, Scott connection method, and the LeBlanc transformer method [8]. Under the regulations of power system regarding the imbalance of a three-phase power system, users of electricity may not apply for UHV single phase power. Therefore, in general, high speed rail system adopts the Scott connection method, whose main transformer's connection system is shown in Fig. 1.

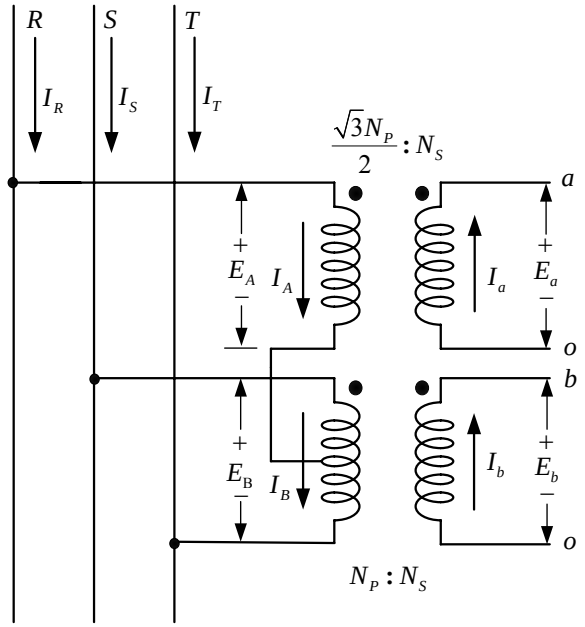

Fig. 1 The connection scheme of the Scott transformer of high speed rail

The equation for the current of the Scott transformer connection method in Fig.1 can be expressed by the following:

$$\frac{E_A}{E_a}=\frac{\sqrt{3}n}{2} \tag{1}$$

$$\frac{E_B}{E_b}=\frac{N_P}{N_S}=n \tag{2}$$

$$I_a=\frac{\sqrt{3}n}{2}I_R \tag{3}$$

$$I_b=nI_B=\frac{n\left(I_S-I_T\right)}{2} \tag{4}$$

Where

E_A and E_B : Primary voltages of the single-phase transformer

E_a and E_b : Secondary voltages of the single phase transformer

N_P : Primary winding turns of the transformer

N_S : Secondary winding turns of the transformer

n : Turn ratio of the transformer

I_a 、I_b : Secondary currents of the transformer

I_R 、I_S 、I_T : Currents of the three-phase power system of the power substation

In order to maintain a balance in a three-phase power system, the current must satisfy the following equation:

$$I_R+I_S+I_T=0 \tag{5}$$

Using the equations from (3) to (5), the relationship between the three phase power current and the two sets of single phase current can be expressed as:

$$I_R=\frac{2}{\sqrt{3}n}\times I_a \tag{6}$$

$$I_S=\left(I_b-\frac{1}{\sqrt{3}}I_a\right)/n \tag{7}$$

$$I_T=-\left(I_b+\frac{1}{\sqrt{3}}I_a\right)/n \tag{8}$$

If the secondary current carried is equal, the equation $|I_R|=|I_S|=|I_T|$ is satisfied, and there is a phase angle difference of 120° , then the system will become a three phase balanced system.

2.2 Structure of the Transformers between the Power Supply Network

In order to decrease the number of power substations and its expenses as well as to reduce the

electromagnetic interference (EMI) on the communication lines, high speed rail uses an auto-transformer connection method as shown in Fig. 2, which increases the voltage of the feed lines and decreases the load current. One set of winding of the auto-transformer connects the tough line to the railway, forming a loop. The other set of winding connects to the current return line from the neural point of the auto-transformer. Most auto-transformers that are used in railway transport systems have tough lines and current returning lines with a standard voltage supply of 50kV. If the winding ratio is 1:1 (number of windings from the railway to the current returning line: number of windings from the tough line to railway), then there will be a voltage of 25kV fed from the tough line to the railway. Increasing the voltage supply or the winding turn ratio can allow for greater distances between power substations. For example, Japan's Tokaido Sanyo Shinkansen uses a winding turn ratio of 2:1. America's Philadelphia railway system uses an auto-transformer winding turns ratio of 3:1. Also, by supplying power research on two sets of high speed railways, the optimal distance between the transformers was found to be between 12-30km [9-11]. High speed railways use the auto-transformer connection method, where the distance between the connection of the supply lines and the transformers is about 10-15 km. This decreases the number of power substations that are required. Furthermore, with the current flowing in opposite directions in the tough lines and current return lines, induced voltage will cancel out, leading to less line interference.

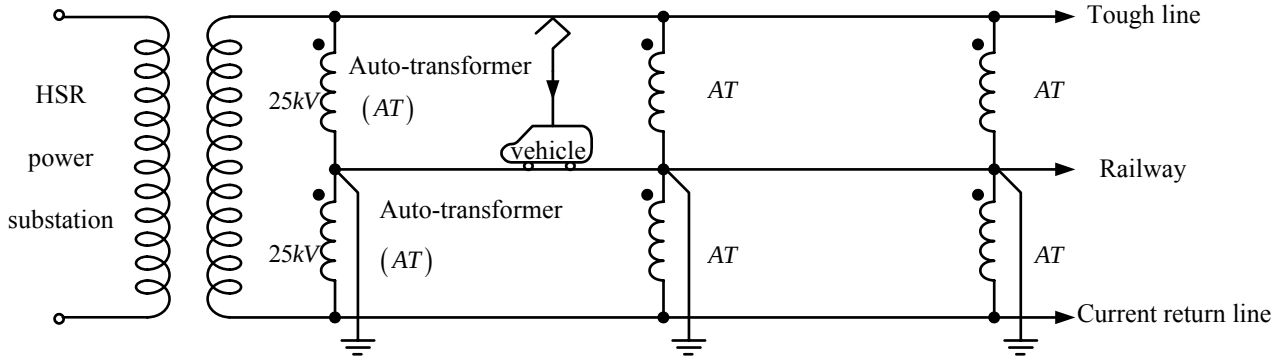

Fig. 2 The auto-transformer connection method adopted by high speed rail

2.3 Analysis of the Equivalent Circuit Model of the Power Supply System Network

Fig. 3 shows the equivalent impedance of the power supply system network and protection lines. By setting railway impedance as Z_r, protection line impedance as Z_{pp}, and the mutual impedance of the lines as equivalent impedance $Z_r^{'}$, the following can be expressed:

$$Z_{pp}I_p + Z_{pr}I_r = Z_rI_r + Z_{pr}I_p = Z_r^{'}I_r^{'} \tag{9}$$

$$I_p + I_r = I_r^{'} \tag{10}$$

I_p represents the current of the protection lines, I_r represents the current of the railways, and $I_r^{'}$ represents the combined current of the protection lines and railways. By inserting (10) into (9), the following can be obtained:

$$I_r = \left(\frac{Z_{pp} - Z_{pr}}{Z_{pp} + Z_r - 2Z_{pr}} \right) I_r^{'} \tag{11}$$

$$I_p = \left(\frac{Z_r - Z_{pr}}{Z_{pp} + Z_r - 2Z_{pr}} \right) I_r^{'} \tag{12}$$

Then, by inserting (11) and (12) back into (10), the equivalent impedance $Z_r^{'}$ of the circuit can be expressed as:

$$Z_r^{'} = \frac{Z_{pp}Z_r - Z_{pr}^2}{Z_{pp} + Z_r - 2Z_{pr}} \tag{13}$$

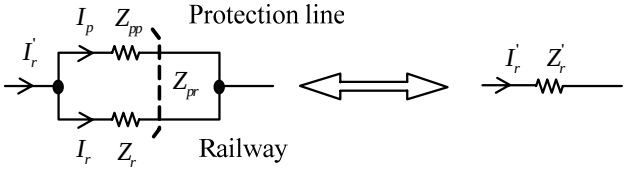

Fig. 3 The equivalent impedance of the protection lines and rails of the power supply system network

Fig. 4 shows the mutual impedance of the power supply system network and railway equivalent impedance. The mutual impedance of the tough line and rails is Z_{tr}, and the mutual impedance of the tough line and protection line is Z_{tp}. Using the Kirchhoff voltage law (KVL) and the Kirchhoff current law (KCL), (14) can be obtained. In addition, the relationship between the mutual impedances of the power supply system network's tough lines and railway equivalent impedance can be expressed as in (15).

$$\frac{Z_{tp}I_t}{Z_{pp}} + \frac{Z_{tr}I_t}{Z_r} = \frac{Z_{tr}^{'}I_t}{Z_r^{'}} \tag{14}$$

$$Z_{tr}^{'} = \left(\frac{Z_{tp}}{Z_{pp}} + \frac{Z_{tr}}{Z_r}\right)Z_r^{'} \tag{15}$$

I_t represents the current of the tough lines.

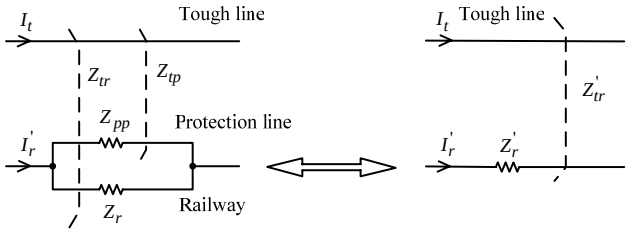

Fig. 4 Mutual impedance of power supply system network's tough lines and railway impedances

Fig. 5 shows the mutual impedance of the power supply system network's current return line and railway equivalent impedances [12-14]. The mutual impedance of the current return line and railway is set as Z_{fr}, and the mutual impedance of the current return line and the protection lines is set as Z_{fp}.

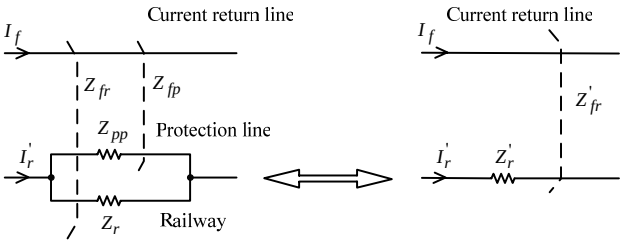

Fig. 5 Mutual impedance of power supply system network's current return line and railway equivalent impedance

Using a similar method of analysis as used above, (16) can be found. In addition, the relationship between the mutual impedances of the power supply system network's current return lines and railway equivalent impedance can be expressed as in (17).

$$\frac{Z_{rp}I_f}{Z_{pp}} + \frac{Z_{fr}I_f}{Z_r} = \frac{Z_{fr}^{'}I_f}{Z_r^{'}} \tag{16}$$

$$Z_{fr}^{'} = \left(\frac{Z_{fp}}{Z_{pp}} + \frac{Z_{fr}}{Z_r}\right)Z_r^{'} \tag{17}$$

2.4 Construction of an Equivalent Circuit Model for the Power Supply System Network

The high speed rail system runs from north to south with several main power substations. The distance between each substation, at most, is 60 kilometers. For the purpose of analyzing high speed rail vehicles' transient response, this paper focuses on high speed rail vehicles within 45 kilometers of the power supply system network's transient behavior. Fig. 6 shows the construction of the high speed rail vehicle's power supply system network and the equivalent circuit.

First, a three-phase 161kV electric voltage is supplied by Power Company, which is then reduced to 50 kV through a Scott transformer. Then, along with an auto-transformer with turn ratio is 1:1. Following this, the voltage is reduced to 25 kV, through the tough line and railway protection line, providing the needed current for the high speed rail vehicle. Every 15 kilometers an auto-transformer is placed, with the auto-transformer providing primary current, and the secondary current transferred back to the high speed rail's power supply system through current return line. Every five kilometers, a railway and protection lines are simultaneously grounded, and along with the actual high speed rail earth system, this completes the high speed rail's power supply system network. The parameters of the high speed rail's power supply system network are presented in Table 1 [12-14]. High speed rail vehicles have a high voltage usage, and in accordance with the laws and regulations, the grounding resistance should be $10\,\Omega$ for special type grounding. Due to the railway and protection line grounding, the equivalent circuit line length shown in Fig. 6 is set as 5 kilometers. In accordance with Table 1 and related data, it is possible to calculate $Z_t = 0.6505+j3.9117\,\Omega$ and $Z_f = 0.78235+j4.50725\,\Omega$, and to obtain the resistance value $Z_r^{'} = 0.5755+j4.56321\,\Omega$ using (13) and the railway and protection line parameters.

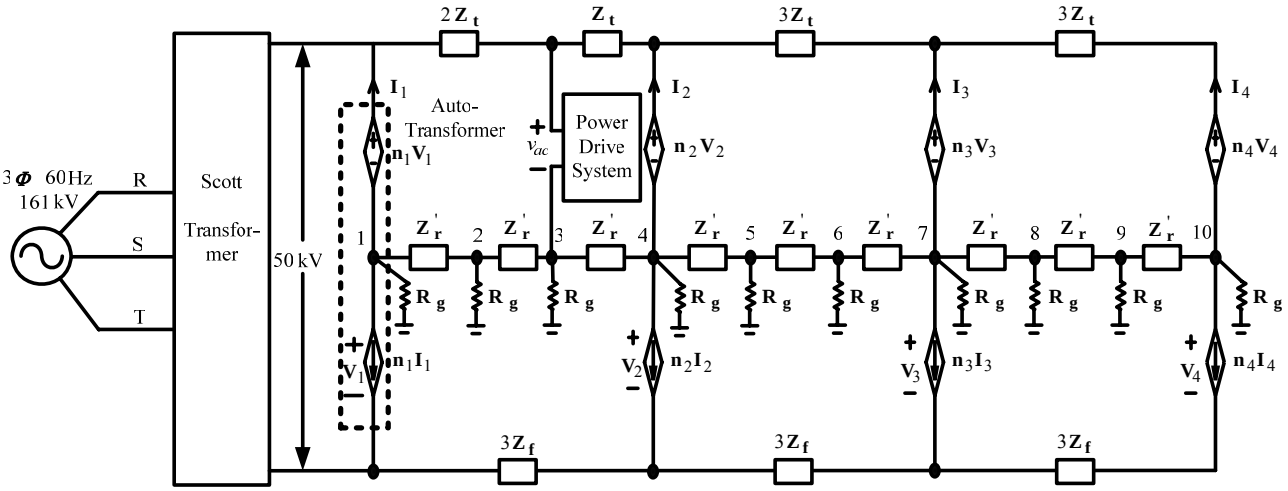

Fig. 6 Constructed equivalent circuit for a power supply system network

Table 1 Parameters regarding the power supply system network of high speed rail vehicles

$Z_r = 0.12815 + j0.68673(\Omega/km)$	$Z_{tr} = 0.05883 + j0.41697(\Omega/km)$
$Z_{pp} = 0.24692 + j0.92700(\Omega/km)$	$Z_{tp} = 0.05843 + j0.44300(\Omega/km)$
$Z_t = 0.13010 + j0.78234(\Omega/km)$	$Z_{fr} = 0.05872 + j0.38956(\Omega/km)$
$Z_f = 0.15647 + j0.90145(\Omega/km)$	$Z_{fp} = 0.05832 + j0.52020(\Omega/km)$
$Z_{pr} = 0.05869 + j0.38134(\Omega/km)$	grounding resistance $R_g = 1\Omega$

3 Structure of High Speed Rail's Traction Power Driving System

Fig. 7 demonstrates the scheme of the proposed high speed rail's traction drive system. Using a three-level neutral point AC/DC converter has two purposes for the power transfer function. First, it allows the high speed rail's vehicle to efficiently use the energy generated during deceleration or braking through feedback to the power supply side. Second, in order to achieve three-level voltage waveform every one and a half periods, a neutral point clamp rectifier formed with eight IGBT power semiconductor switches ($S_1 - S_8$) and four clamping diodes ($D_1 - D_4$) was constructed. In the AC source side, a boosting inductor is connected with the vehicle transformer's secondary side, which acts as the power control's energy storage inductor. The converter's DC side is connected to capacitors C_1 and C_2, and through the DC voltage controller, the converter's DC capacitors and DC-link provide a stable DC voltage. Then, after going through the DC-link voltage controller, the error between the DC-link feedback voltage $V_{dc}^{'}$ ($= K_v V_{dc}$, K_v represents the voltage sensed factor) and command voltage V_{dc}^{*} produce a peak command current $\hat{I}_{ac}^{*}$. By multiplying this with the unit sine wave $S(\omega t)$ of the power supply voltage, the input command current i_{ac}^{*} can be found. Finally, by using a hysteresis current controller (HCC) to create a switching signal for a semiconductor switch, the actual input current $i_{ac}^{'} = K_s i_{ac}$ (K_s represents the current sensed factor) can be made to follow the command current i_{ac}^{*} tightly. In addition, a neutral point voltage compensator can be used to solve the problem of a current imbalance in two DC-link capacitors.

Fig.7's three-level converter electric circuit is constructed through the use of 12 power semiconductor switches and 6 neutral point clamped

diodes. Every four semiconductor switches are connected with a reverse clamped diode and two neutral point clamped diodes, in order to prevent short-circuiting when the power is switched on and off. The switch's signal choices are labeled as $S_{i1} = \overline{S_{i3}}$ and $S_{i2} = \overline{S_{i4}}$ (of which exists $i = 1,2,3$) with every two making up a set. Every switch component is able to deliver a control signal because of what the indirect-field-oriented mechanism generates, which is the error comparison between three phase current command i^*_{abc} and actual phase current $i^{'}_{abc}$ generated. Then, through a current controller, it generates three-phase controlled voltage signals to compare with two triangular wave forms. After this, it then decides whether to switch on to generate activity, using the actual current to track its current command, and then engage in giving the high speed rail vehicle its needed required speed [15].

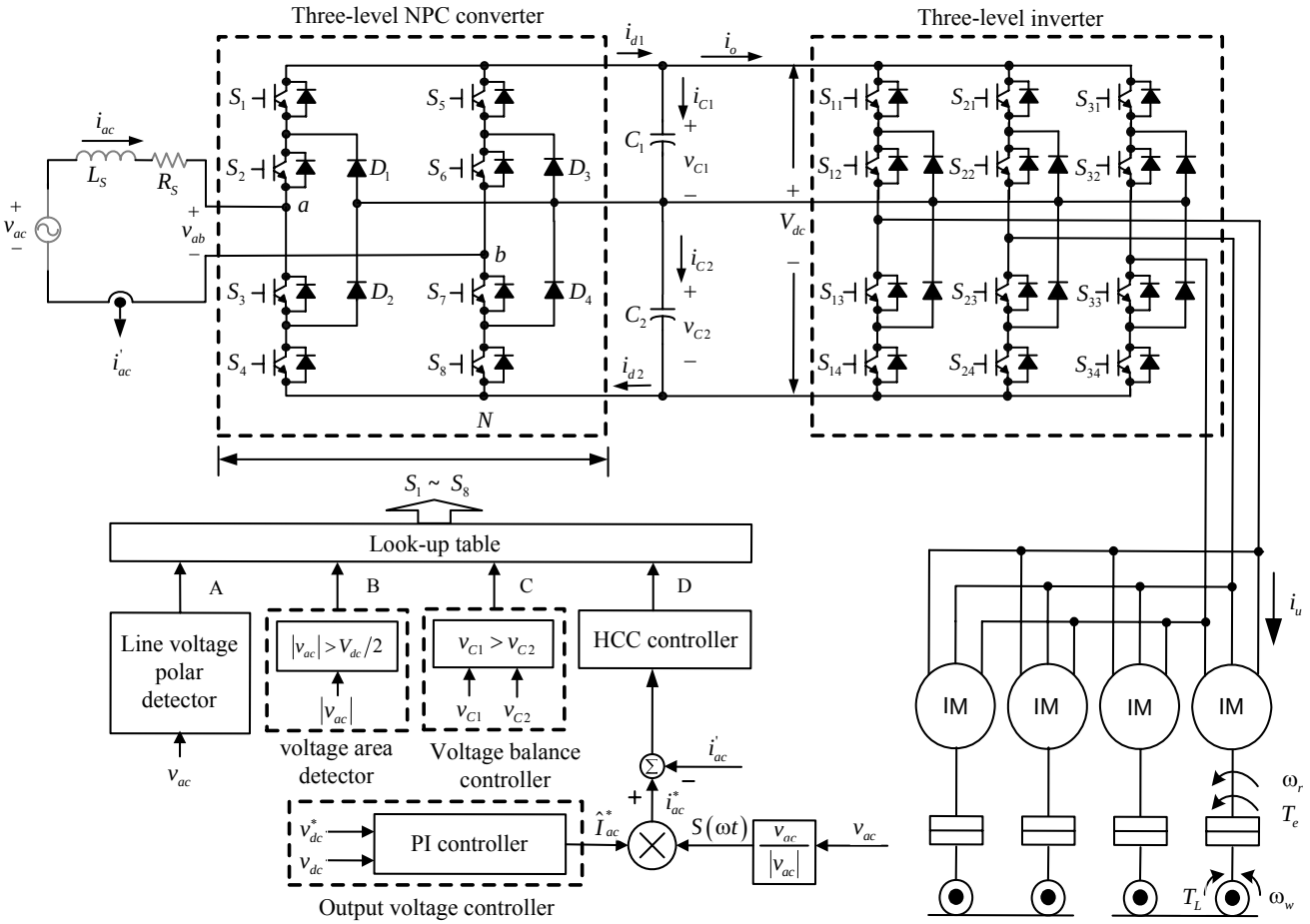

Fig. 7 Structure of high speed rail's traction power driving system

4 Simulation Results

The paper utilizes PSIM software to construct Fig. 6 to demonstrate high speed rail's vehicle power system supply network and equivalent circuits. Combined with what is shown in Fig. 7, which shows power traction system, a traction power driving simulation was conducted. The simulation of high speed rail's system during its change in speed and the conditions are shown in Fig. 8. From the simulation results, it is clear that the high speed rail vehicle demonstrates a stabilized performance when it is initially in a non-moving state and then sped up to its designed train speed (300 km/hr). At the same time of the change in speed, the power supply system network can be observed to have been affected by the change in speed. Fig. 9 shows the grounding current leakage simulation results of the power supply system network. The simulation results indicate that there is a great current leakage at vehicle's present grounding position, because of the vehicle's power is supplied between the touch line and rail and the rail acts as a power circuit route. Fig. 10 shows the AC side voltage v_{ac} and current i_{ac} waveforms during vehicle's acceleration and deceleration. The simulation results show that in the instant the rail reduces its speed, the high speed rail vehicle's traction power driving motor is able to transfer energy to the AC power side, which allows the input current to rapidly change.

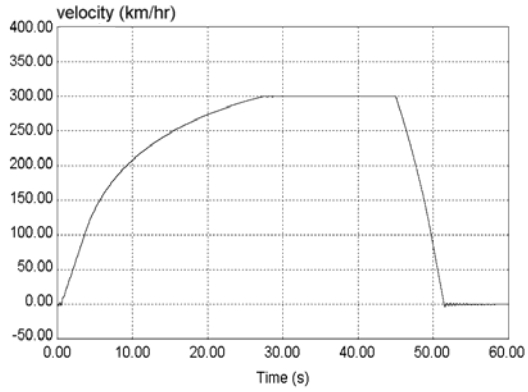

Fig. 8 State of high speed rail vehicle during change of speeds

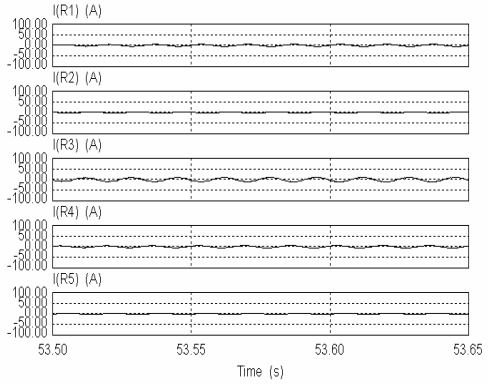

(a)

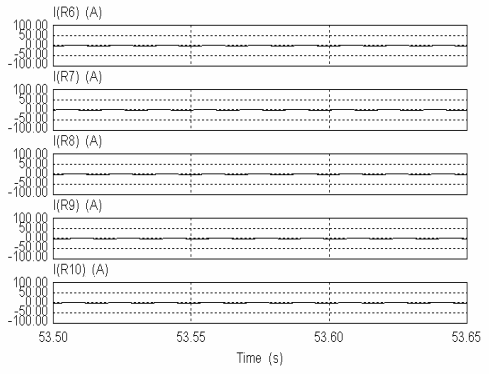

(b)

Fig. 9 High speed rail vehicle's change in speed and the power supply system network's current leakage simulation results: (a) grounding point from 1 to 5; (b) grounding point from 6 to 10

Fig.11 and Fig.12, respectively, show the high speed rail vehicle's wave forms of the input AC voltage and AC current, along with the DC voltage during its initial stage of acceleration. In the beginning stages of the simulation, the input current of AC voltage and AC current are in phase, with the power factor close to 1. At this time the DC voltage, due to the increase in speed, the traction power driving motor generates a large electrical current, causing the DC voltage to decrease. From Fig. 13 and Fig. 14, the simulation vehicle displays results that changes the load momentum inertia, and uses the energy that was generated through the converter to transfer it back to the AC electrical source. This causes the DC voltage to rise to 4,222V, which makes the input AC current no longer a sine wave. Hence, there is a sudden jump in its harmonic components. By this time, the input AC voltage and AC current are no longer in phase. From Fig.15, it can be observed that at the last stage of the high speed rail vehicle speed reduction, the power supply input of AC voltage and AC current sine wave are negatively correlated, which means that the traction power drive system and other control systems can indeed efficiently transfer energy back to the electrical power system.

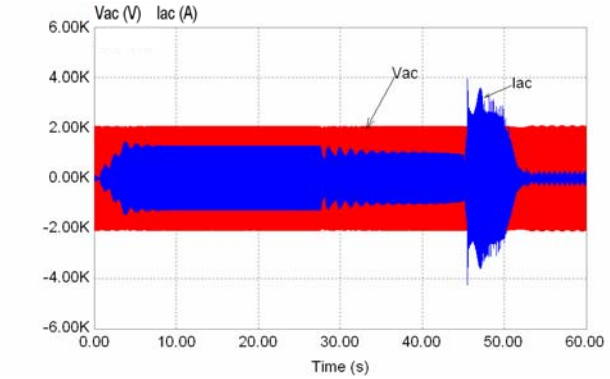

Fig. 10 The input voltage and current's wave forms due to speed change of high speed rail vehicle

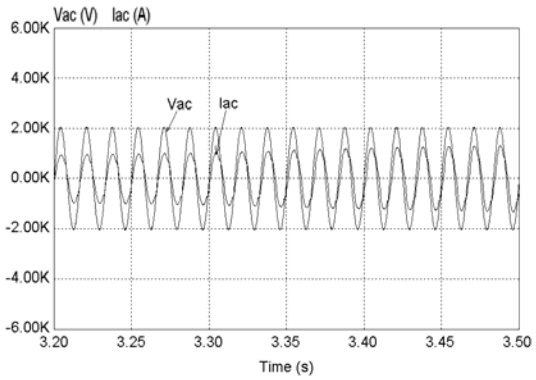

Fig. 11 AC voltage and AC current wave forms during high speed rail vehicle's acceleration during its initial change in speed

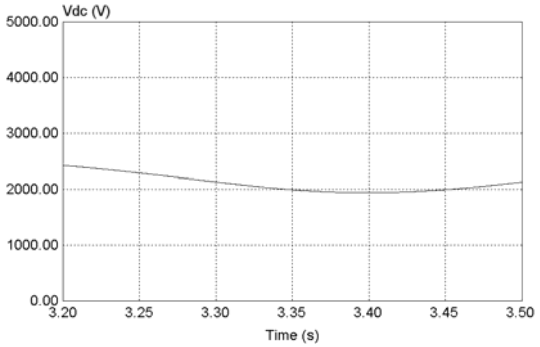

Fig. 12 High speed rail vehicle's DC voltage wave form during acceleration stage

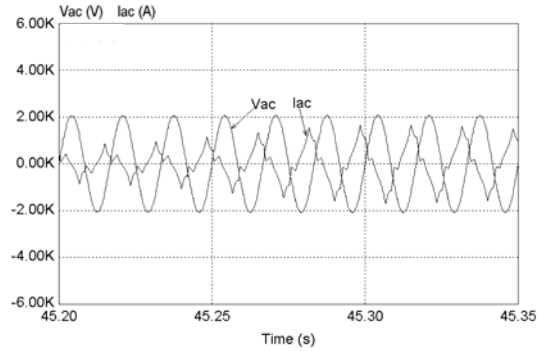

Fig.13 High speed rail vehicle's input AC voltage and AC current waveforms during initial stage of deceleration

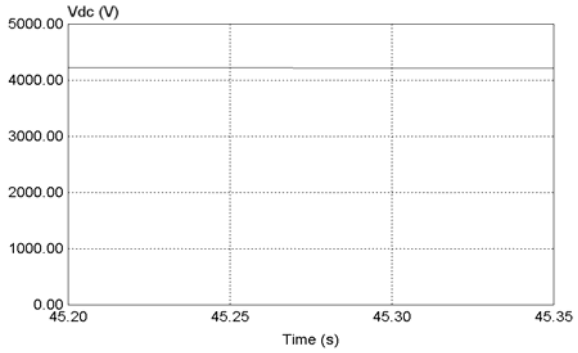

Fig. 14 High speed rail vehicle's DC voltage wave forms during initial stage of deceleration

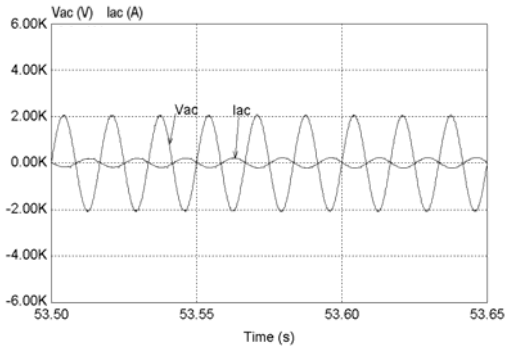

Fig. 15 High speed rail vehicle's AC voltage and AC current wave forms during final stage of deceleration

The largest current leakage of grounding during the high speed rail vehicle's change in speed is shown in Table 2. As shown in the table, the position of the vehicle (at grounding point 3) shows the greatest current leakage, and the intervals of current leakage slowly decrease thereafter. During the change in speed, it can be observed that the initial deceleration causes the grounding potential to sharply increase as shown in Fig. 16.

According to the simulation results, the high speed rail vehicle's change in speed does have an effect on the power supply system network and the traction power drive system. Through analysis, it is known that during the initial stages of deceleration, DC voltage sharply increases, which causes a great amount of current leakage. This furthers the rise in earth potential, and if the voltage is greater than what the rail can undertake, it will produce electrical arc erosion to the rail, decreasing the lifespan of the rail, which will increase the cost of operations and the severe damage of the high speed rail system.

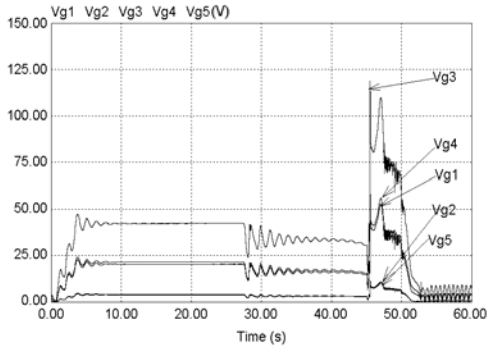

(a)

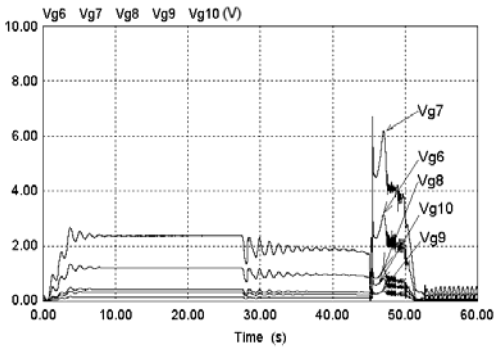

(b)

Fig. 16 State of rise in earth potential of railway in relation with high speed rail vehicle's power supply system network and change in speed: (a)grounding point 1 through 5; (b)grounding point 6 through 10

Table 2 Various stages of high speed rail change in speed and the grounding current leakage value

Grounding Point Current	Initial Stage of Acceleration (A)	Middle Stage of Acceleration (A)	Initial Stage of Deceleration (A)	Final Stage of Acceleration (A)
I(R1)	31.4	29.78	37.08	5.33
I(R2)	6.14	6.06	6.40	1.08
I(R3)	67.12	61.74	79.64	11.30
I(R4)	36.05	32.58	38.08	5.86
I(R5)	5.85	5.68	6.07	1.02
I(R6)	1.74	1.72	1.70	0.31
I(R7)	3.54	3.39	3.70	0.62
I(R8)	0.63	0.62	0.62	0.11
I(R9)	0.21	0.21	0.20	0.04
I(R10)	0.46	0.45	0.43	0.08

5 Conclusion

This paper uses PSIM software to construct the high speed rail's power traction drive system, which includes the Scott transformer, auto-transformer, and rail and equivalent electrical circuits and grounding system. In addition to using a rail equivalent circuit, power grid system and power traction drive system, it can be determined that there is a current leakage effect on the vehicle's transient response behavior. From the simulation results, the vehicle was demonstrated to have a great increase in grounding potential due to the dramatic change in DC voltage from the current leakage during the vehicle's deceleration. The simulation result of this paper can provide valuable assistance to High Speed Rail Company.

6 Acknowledgement

This work was supported by the National Science Council, Taiwan, R.O.C., under the Grant of # NSC-96-2221-E-167-012.

References

[1] T. H. Chen and Y. F. Hsu, "Systematized Short-Circuit Analysis of a 2x25kV Electric Traction Vehicle," *Electric Power Systems Research*, Vol. 47, No. 2, 1998, pp. 133-142.

[2] J. G. Yu and C. J. Goodman, "Modeling of Rail Potential Rise and Leakage Current in DC Rail Transit Systems," *IEE Colloquium on Stray Current Effects of DC Railways and Tramways*, 1990, pp. 2/2/1-2/2/6.

[3] F. Dawalibi, "Grounding Fault Current Distribution between TSoil and Neutral Conductors," *IEEE Transactions on Power Apparatus and Systems*, Vol. 99, No. 2, 1980, pp. 452-461.

[4] E. Zhong and T. A. Lipo, "Improvements in EMC Performance of Inverter-Fed Motor Drives," *IEEE Transactions on Industry Applications*, Vol. 31, No. 6, 1995, pp. 1247-1256.

[5] M. A. EI-Kady and M. Y. Vainberg, "Risk Assessment of Grounding Hazards Due to Step and Tough Potentials near Transmission Line

Structure," *IEEE Transactions on Power Apparatus and Systems*, Vol. 102, No. 93, 1983, pp. 3080-3087.

[6] S. T. Sobral, C. A. O. Peixoto and D. Mukhedlkar, "Grounding Potential Distribution in the Neighberhood of the Itaipu Generation Complex," *IEEE Transactions on Power Delivery*, Vol. 1, No. 1, 1986, pp. 85-91.

[7] S. H. Lee and C. M. Liaw, "Modeling and Quantitative Direct Digital Control for a DSP-based Soft-Switching Rectifier," *IEE Proceeding: Electric Power Application*, Vol. 150, No.1, 2003, pp. 21-30.

[8] T. H. Chen, "Comparison of Scott and Leblanc Transformers for Supplying Unbalanced Electric Railway Demands," *Electric Power Systems Research*, Vol. 28, No. 3, 1994, pp. 235-240.

[9] R. J. Hill and I. H. Cevik, "On-Line Simulation of Voltage Regulation in Autotransformer-Fed AC Electric Railroad Traction Networks," *IEEE Transactions on Vehicular Technology,* Vol. 42, No. 3, 1993, pp. 365-372.

[10] R. J. Hill, "Electric Railway Traction, Part III-Traction Power Supplies," *Power Engineer Journal*, Vol. 8, No. 6, 1994, pp. 275-286.

[11] R. E. Morrison, "Parameters that Influence Industrial Frequency AC Power Quality on Traction Systems," *in Proceedings of Power Engineering Society Summer Meeting*, Vol. 1, 2001, pp.204-209.

[12] S. Wall and R. Jackson, "Fast Controller Design for Practical Power-Factor Correction Systems," *IEEE Transactions on Industrial Electronics,* Vol. 44, No.5, 1997, pp. 1027-1032.

[13] R. J. Hill and D. J. Carpenter, "Rail Track Transmission Line Distributed Impedance and Admittance: Theoretical Modeling and Experimental Results," *IEEE Transactions on Vehicular Technology*, Vol. 42, 1993, pp. 225-241.

[14] R. J. Hill and D. J. Carpenter, "Determination of Rail Internal Impedance for Electric Railway Traction System Simulation," *IEE Proceedings-B*, Vol. 138, No. 6, 1991, pp. 311-321.

[15] C. H. Cheng, K. H. Chao and P. Y. Chen, "Modeling and Quantitative Design of a Three-Level PWM Converter with Power Factor Correction," *in Proceedings of the 27th ROC Symposium on Electrical Power Engineering,* 2006, pp. PA3.14.1-PA3.14.5.